1-1-2012

Synthesis and electrochemical properties of Sn-SnO2/C nanocomposite

Chuanqi Feng
Hubei University, China, cfeng@uow.edu.au

Meiyu Dan
Hubei University

Chaofeng Zhang
University of Wollongong, czhang@uow.edu.au

Zaiping Guo
University of Wollongong, zguo@uow.edu.au

Shiquan Wang
Hubei University

See next page for additional authors

Synthesis and electrochemical properties of Sn-SnO2/C nanocomposite

Abstract

A Sn-Sn02/C nanocomposite was synthesized using the electrospinning method. Thermal analysis was used to determine the content range of Sn and Sn02 in the composite. The composite was characterized by X-ray diffraction, and the particle size and shape in the Sn-SnOiC composite were determined by scanning and transmission electron microscopy. The results show that the Sn-Sn02/C composite takes on a nanofiber morphology, with the diameters of the nanofibers distributed from 50 to 200 nm. The electrOChemical properties of the Sn-SnOiC composite were also investigated. The Sn-SnOiC composite as an electrode material has both higher reversible capacity (887 mAh· g-I). and good cycling performance in lithium-anode ceUs working at room temperature in a 3.0 V to O.Ot V potential window. The Sn-Sn02/C composite could relain a discharge capacity of 546 mAWg aller 30 cycles. The outstanding electrochemical properties of the Sn-SnOiC composite oblained by this method make it possible for Ihis composite to be used as a promising anode material.

Keywords

nanocomposite, c, electrochemical, sno2, synthesis, sn, properties

Disciplines

Engineering | Science and Technology Studies

Publication Details

Feng, C., Dan, M., Zhang, C., Guo, Z., Wang, S. & Zeng, R. (2012). Synthesis and electrochemical properties of Sn-SnO2/C nanocomposite. Journal of Nanoscience and Nanotechnology, 12 (10), 7747-7751.

Authors

Chuanqi Feng, Meiyu Dan, Chaofeng Zhang, Zaiping Guo, Shiquan Wang, and R Zeng

Journal of
Nanoscience and Nanotechnology
Vol. 12, 7747–7751, 2012

Synthesis and Electrochemical Properties of Sn–SnO_2/C Nanocomposite

Chuanqi Feng[1,*], Meiyu Dan[1], Chaofeng Zhang[2], Zaiping Guo[2], Shiquan Wang[1], and R. Zeng[3]

[1] *Key Laboratory for Functional Materials and Green Synthesis of the Ministry of Education, Hubei University, Wuhan 430062, P. R. China*
[2] *School of Mechanical, Materials and Mechatronic Engineering, University of Wollongong, NSW 2522, Australia*
[3] *Solar Energy Technologies, School of Computing, Engineering and Mathematics, University of Western Sydney, Penrith Sout, Sydney, NSW 2751, Australia*

A Sn–SnO_2/C nanocomposite was synthesized using the electrospinning method. Thermal analysis was used to determine the content range of Sn and SnO_2 in the composite. The composite was characterized by X-ray diffraction, and the particle size and shape in the Sn–SnO_2/C composite were determined by scanning and transmission electron microscopy. The results show that the Sn–SnO_2/C composite takes on a nanofiber morphology, with the diameters of the nanofibers distributed from 50 to 200 nm. The electrochemical properties of the Sn–SnO_2/C composite were also investigated. The Sn–SnO_2/C composite as an electrode material has both higher reversible capacity (887 $mAh \cdot g^{-1}$) and good cycling performance in lithium-anode cells working at room temperature in a 3.0 V to 0.01 V potential window. The Sn–SnO_2/C composite could retain a discharge capacity of 546 mAh/g after 30 cycles. The outstanding electrochemical properties of the Sn–SnO_2/C composite obtained by this method make it possible for this composite to be used as a promising anode material.

Keywords: Tin Oxide, Anode Material, Electrospinning, Electrochemical Properties.

RESEARCH ARTICLE

1. INTRODUCTION

Tin oxide compounds are most noted for their low potentials for Li^+ insertion and high storage capacities as anode materials,[1–4] although poor cycling stability limits their application in the lithium ion battery field. Such material deficiency is due to the large specific volume changes during Li^+ insertion and extraction reactions, which cause electrode disintegration. Several research groups have reported that doping tin oxide compounds with carbon could ease the capacity fading.[5–8] It is believed that the particle size, the type of composite, and its morphology are important factors that affect the material performance.[9–13] In this paper, the synthesis of a Sn–SnO_2/C nanofiber composite by the electrospinning method is reported for the first time, and the electrochemical properties have also been investigated. This provides both a theoretical basis and an experimental foundation for developing the uses of Sn–SnO_2/C composite in applications for the lithium ion battery industry.

2. EXPERIMENTAL DETAILS

The raw materials, $Sn(C_{16}H_{30}O_4)$, polyacrylonitrile (PNA) (molecular weight 1.5×10^6), and the organic solvent dimethylformamide (DMF) were Analytical Reagent (AR) grade. In a typical procedure, 0.85 g $Sn(C_{16}H_{30}O_4)$ was dissolved in 4 g DMF to form solution (A), 0.7 g PNA was added into 10 g DMF and heated at 60 °C to form a transparent solution (B). Solution (A) and solution (B) were mixed together under vigorous stirring for 2 h to form solution (C). The ratio of $Sn(C_{16}H_{30}O_4)$ and PNA in DMF can control the ratio of Sn and C in composite. An appropriate amount of solution (C) was taken up in a 10 ml glass syringe, which was then placed on a syringe pump. After applying 16 kV electric potential between the metallic syringe-tip and the plate (with a 12 cm distance between them), the mixed solution (C) was continuously fed to the syringe-tip, which had an inner diameter of 0.8 mm, at the constant flow rate of 1 ml/h using the syringe pump. The plate was covered by nickel foam to act as a collector, and its temperature was controlled at 250 °C (see Fig. 1).

*Author to whom correspondence should be addressed.

 1533-4880/2012/12/7747/005 doi:10.1166/jnn.2012.6659

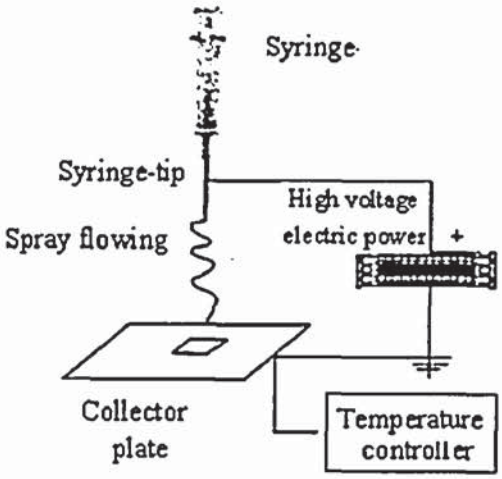

Fig. 1. Electrospinning system.

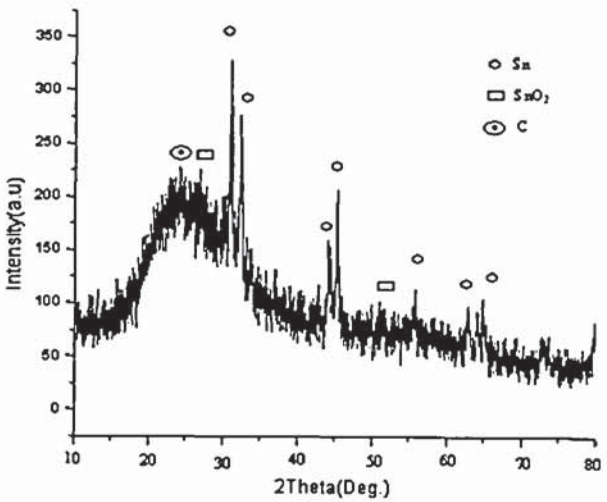

Fig. 2. XRD pattern of Sn–SnO_2/C composite.

The precursor film was moved to a furnace and heated at 550 °C for 6 h under flowing Ar gas to yield a blocky composite. The blocky composite was ground to form powder. The composite powder was characterized by scanning electron microscopy (SEM, JEOL JSM 6460A) and transmission electron microscopy (TEM, Philip, Technai), as well as X-ray diffraction (XRD, Shimadzu XRD-6000).

The electrochemical characterizations were performed using coin cells (CR2016). The electrode was prepared by dispersing 60 wt% as-prepared powders and 30 wt% carbon black in 10 wt% polytetrafluoroethylene (PTFE) solution. The as-prepared powder and carbon black powder were first added to a solution of PTFE in isopropanol to form a homogeneous slurry. The slurry was then spread onto nickel foil. The coated electrodes were dried at 125 °C for 24 hours in vacuum and then pressed to enhance the contact between the active materials and the conductive carbon. Coin test cells were assembled in an argon filled glove box, where the counter electrode was Li metal and the electrolyte was 1 mol/L $LiPF_6$ dissolved in a 50/50 vol% mixture of ethylene carbonate (EC) and diethyl carbonate (DEC). These cells were galvanostatically charged and discharged in the voltage range of 0.01 to 3.0 V at room temperature to measure the electrochemical response. The current density used was 40 mA/g.

3. RESULTS AND DISCUSSION

3.1. Structure and Morphology Characterization

The XRD pattern of the as-prepared sample is shown in Figure 2 In the pattern of the Sn–SnO_2/C composite, all the peaks can be assigned to Sn, SnO_2, and C. This indicates that the precursor was decomposed completely to form the Sn, SnO_2, and C composite. From Figure 2, it can be seen that the composite mainly contains non-crystalline C and Sn, as well as little non-crystalline SnO_2. This proves that the precursor containing $Sn(C_{16}H_{30}O_4)$ and PNA was decomposed to form Sn, SnO_2, C, H_2O, and other smaller molecule hydrocarbon compounds (such as CH_4, C_2H_6 and so on) under Ar atmosphere.

The thermogravimetric analysis (TGA) and differential thermal analysis (DTA) curves of the Sn–SnO_2/C composite under air atmosphere are shown in Figure 3. It can be seen that from 400 to 607 °C, the carbon was oxidized to form CO_2, while the Sn in the composite was oxidized to form SnO_2, resulting in two exothermic peaks, which overlapped to form a single broad peak, as shown in the DTA curve. The chemical reaction is as follows:

$$Sn + C + 2O_2 \rightarrow SnO_2 + CO_2$$

In the TGA curve, if the content of Sn in the composite is much higher than that of SnO_2, that is, the initial SnO_2 content in the composite is negligible, total weight of SnO_2 in the product was resulted from the combustion of Sn in the composite. According to the relevant data, the content of Sn in composite could then be calculated as 19.6% (The content of SnO_2 in composite is 24.91% observed from Fig. 3), and the content of carbon would be about 80.4%. If the content of SnO_2 in the composite is much higher than that of the Sn and the initial Sn content

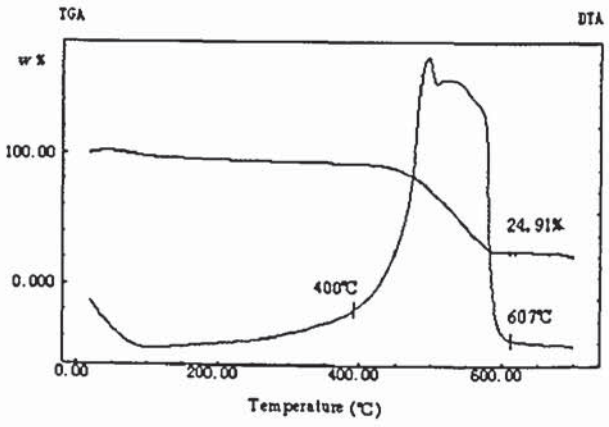

Fig. 3. TGA-DTA curves of Sn–SnO_2/C composite.

RESEARCH ARTICLE

in the composite is negligible, the loss of weight is solely attributable to the combustion of carbon, so that the carbon content would be 75.09% and the SnO_2 content would be 24.91%. However, the composite contains both Sn and SnO_2, so that we can safely assume that the total content of Sn and SnO_2 in the composite is in the range of 19.6 to 24.91% wt.

X-ray photoelectron spectroscopy (XPS) results on the sample are shown in Figure 4. From Figure 4, it can be found that the $3d_{5/3}$ and $3d_{3/2}$ binding energy peaks are resulted from the overlap of two peaks for Sn and Sn^{4+} binding energy, which proves also that the composite contained Sn and SnO_2. (The $3d_{5/3}$ binding energy of Sn is about 485 eV, and the $3d_{5/3}$ binding energy of SnO_2 is about 486.8 eV.)

Figure 5 shows a typical SEM (a) and TEM (b) image of the as-prepared Sn–SnO_2/C composite. It can be observed that the Sn–SnO_2/C composite has taken on a nanofiber morphology, with the diameters of the nanofibers distributed from 50 to 200 nm.

When the Sn–SnO_2/C composite was ground, it still retained the nanofiber morphology. See TEM (b). The diameters of the nanofibers observed are in agreement with those determined from SEM (a). By energy dispersive spectroscopy (EDS) analysis (not shown), the content of Sn in the composite was found to be 20.1 wt%, which is exactly in the range of 19.6 to 24.91 wt% obtained by thermal analysis. Our assumption is proved further that the Sn content in the composite is much greater than that of the SnO_2 in the composite.

3.2. Electrochemical Properties

The electrochemical properties of the as-prepared electrodes were measured via coin cell testing. Figure 6 shows the charge/discharge profiles of the as-prepared electrodes. In Figure 6, two lithium insertion plateaus at ~1.0 and ~0.6 V, as well as a slope starting from 0.5 V and running down to the cut-off voltage of 0.01 V, were observed in the first discharge curve. From the second cycle, the discharge plateau is located at about 0.6 V, while the

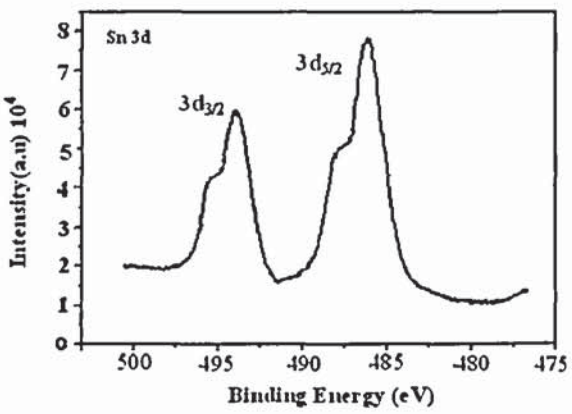

Fig. 4. XPS spectrum of Sn–SnO_2/C composite.

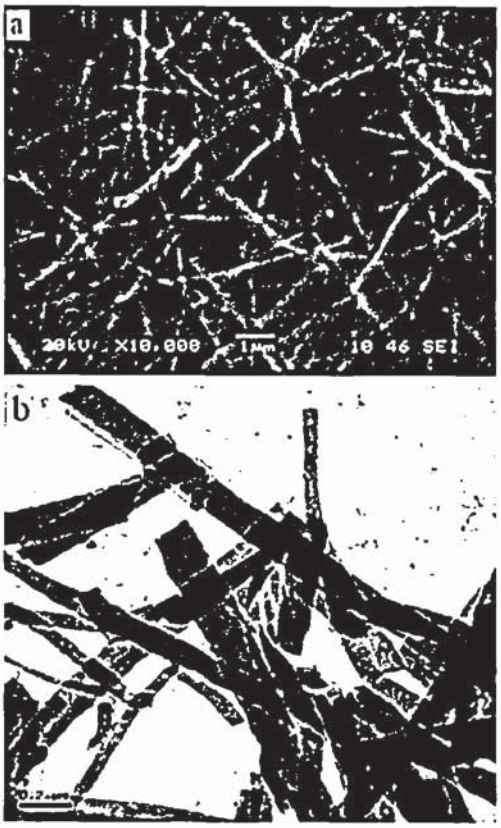

Fig. 5. SEM (a) and TEM (b) image of Sn–SnO_2/C composite.

discharge plateaus at higher potential observed in the first cycle have disappeared. In the charge curve, lithium ion de-intercalation plateaus appeared at ~1.0 V. Based on the above analysis, the relevant reactions are as follows:

Discharging process:

$SnO_2 + 4Li^+ + 2e^- \rightarrow 2Li_2O + Sn$ (1) $E = 3.0 \sim 1.0$ V

$Sn + xLi^+ + xe^- \rightarrow Li_xSn$ $(0 < x < 4.4)$ (2) $E = 0.6 \sim 0.4$ V

$C + xLi^+ + xe^- \rightarrow Li_xC$ (3) $E = 0.4 \sim 0.01$ V

Charging process:

$Li_xC \rightarrow C + xLi^+ + xe^-$ (4) $E = 0.01 \sim 0.6$ V

$Li_xSn \rightarrow Sn + xLi^+ + xe^-$ (5) $E = 0.6 \sim 3.0$ V

The initial discharge capacity was 1328.5 mAh/g and the second discharge capacity was 887.4 mAh/g. The large loss of initial discharge capacity resulted from the irreversibility of reaction (1) and the solid electrolyte interphase (SEI) formation.[14]

It is suggested that, in the first lithiation process, redox reactions occurred between SnO_2 and Li at high potentials (2.0~1.0 V), and then lithium ions were intercalated into Sn (0.6~0.4 V) and intershell van der Waals spaces in the nanofibers at low potentials (0.4~0.01 V). During the charging process, lithium ions first de-intercalate from the carbon in nanofibers at lower potentials around 0.1~0.6 V, and then redox reactions occur at higher potentials (0.6~3.0 V) within this potential range, with a plateau

RESEARCH ARTICLE

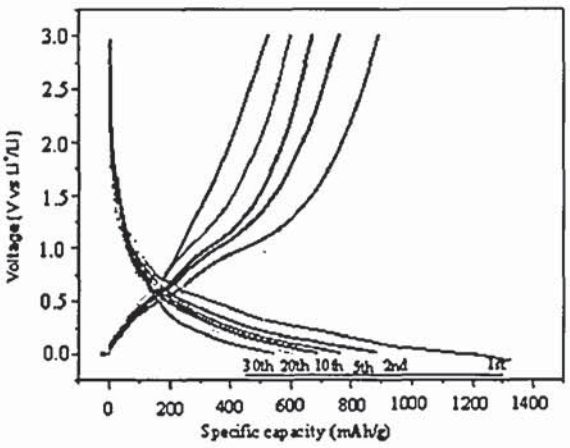

Fig. 6. Typical charge and discharge curves for Sn–SnO_2/C composite at selected cycles.

observed around 1.0 V on the charging curves. In these redox reactions, Li_xSn was reacted to produce Sn and Li^+.

The cycling performance of the as-prepared electrode is presented in Figure 7. The initial discharge capacity of the Sn–SnO_2/C composite is 1328.5 mAh/g at the current density of 40 mA/g. From the first cycle to the second cycle, the loss of discharge capacity is remarkable, but the electrode then maintained stable cycling performance with continuous cycling (with of a loss of capacity of nearly 0.7% per cycle). This is because of the high conductivity of the Sn–SnO_2/C composite nanofibers, which cause the utilization efficiency of Sn–SnO_2 to be improved. In addition, carbon in the nanofibers as an active anode material, also make some contribution to capacity, so Sn–SnO_2/C composite nanofibers exhibit higher capacity in this situation where the content of pure Sn and SnO_2 in the composite is in the range from 19.6 to 24.91 wt%. The Sn–SnO_2/C composite nanofibers have particularly good cycling performance. After 30 cycles, the discharge capacity of Sn–SnO_2/C composite nanofibers still remained at about 546 $mAh \cdot g^{-1}$. During the process of charging and discharging, non-crystalline C in the composite nanofibers played a key role in the cycling performance of the composite. According to the literature[2] and our own knowledge, the electrode reactions of Sn and SnO_2 are as described in the above chemical reactions (1) and (2). There are several factors that affect the cycling performance, such as pulverization of the active particles during charge and discharge, and poor conductivity of the active materials (Sn and SnO_2). To prevent the pulverization during the charge–discharge cycle and improve the conductivity, an effective method is to form a composite with carbon. In the Sn–SnO_2/C nanofiber composite, the C in the nanofiber composite can act as a barrier to suppress the aggregation and pulverization of active particles (Sn–SnO_2) and thus increase their structural stability during cycling. Furthermore, the Sn–SnO_2/C composite nanofibers have high electronic conductivity and can improve the conductance of the active materials. In addition, carbon in the composite is also an active material, so it offers extra capacity. Considering the high reversible capacity and good cycling stability of the as-prepared Sn–SnO_2/C composite nanofiber to compare with pure Sn or SnO_2, electrode, Sn–SnO_2/C composite nanofibers could be a promising alternative anode material for lithium ion batteries.[15]

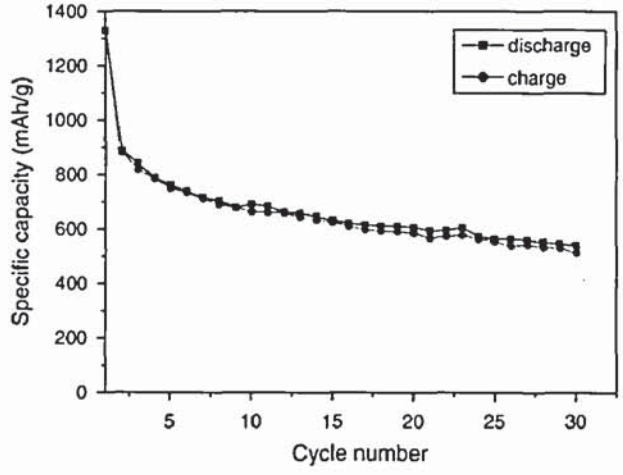

Fig. 7. Relationship between the discharge capacity and cycle number.

4. CONCLUSIONS

In this study, Sn–SnO_2/C nanocomposite was synthesized using the electrospinning method. The Sn–SnO_2/C composite takes on a nanofiber morphology, with the diameters of the nanofibers distributed from 50 to 200 nm. The synthesized composite shows stable cycle performance over a wide voltage range. The reversible capacity after 30 cycles for the composite is about 546 mAh/g. These improvements can be attributed to the particular morphology of the composite (nanofibers) in wich the distance for lithium ions to be inserted in or de-intercalated became shorter and the electrode polarization was decreased. The C in the composite nanofibers could act as a barrier to suppress the aggregation and pulverization of Sn particles and thus increase its structural stability during cycling, as well as keeping the particles electrically connected and thus giving the Sn–SnO_2/C nanomaterial better electrochemical performance compared with Sn or SnO_2. In addition, lithium ions could be intercalated and de-intercalated into the carbon in the composite nanofibers, which makes a partial contribution to the capacity of the composite. So, the Sn–SnO_2/C composite is a promising candidate anode material for lithium ion battery applications.

Acknowledgments: Financial support provided by the Australian Research Council (ARC) through an ARC Discovery project (DP0878611) and the International Cooperation Project of Hubei Provincial Science and Technology Department (No. 2011BFA002) is gratefully acknowledged.

RESEARCH ARTICLE

References and Notes

1. P. Poizot, S. Laruelle, and S. Grugeon, *Nature* 407, 496 (2000).
2. P. Poizot, S. Laruelle, S. Grugeon, and J.-M. Tarascon, *J. Electrochem. Soc.* 149, A1212 (2002).
3. M. Dolle, P. Poizot, and L. Dupont, *Electrochem. Solid-State Lett.* 5, A18 (2002).
4. G. X. Wang, Y. Chen, K. Konstantinov, M. Lindsay, H. K. Liu, and S. X. Dou, *J. Power Sources* 109, 142 (2002).
5. S. Iijima, *Nature* 354, 56 (1991).
6. P. Poizot, S. Laruelle, S. Grugeon, and J.-M. Tarascon, *J. Power Sources* 97/98, 235 (2001).
7. D. Larcher, G. Sudant, and J. B. Leriche, *J. Electrochem. Soc.* 149, A234 (2002).
8. X. H. Huang, J. P. Tu, and B. Zhang, *J. Power Sources* 161, 541 (2006).
9. A. Débart, L. Dupont, P. Poizot, and J.-B. Leriche, *J. Electrochem. Soc.* 148, A1266 (2001).
10. K. T. Lee, Y. S. Jung, and S. M. Oh, *J. Am. Chem. Soc.* 125, 5652 (2003).
11. J. Fan, T. Wang, C. Yu, B. Tu, Z. Jiang, and D. Zhao, *Adv. Mater.* 16, 1432 (2004).
12. L. J. Fu, H. Liu, H. P. Zhang, C. Zhang, T. Li, and Y. P. Wu, *Electrochem. Commun.* 8, 1 (2006).
13. W. Yong, F. Su, G. X. Zhao, and J. Y. Lee, *Chem. Mater.* 18, 1347 (2006).
14. C. Q. Feng, L. Li, Z. P. Guo, and H. Li, *Journal of Alloys Compd.* 504, 457 (2010).
15. N. Catarina, S. Raphaël, W. Patrick, and B. Denis, *Energy Convers. Manage.* 56, 32 (2012).

Received: 8 June 2012. Accepted: 15 July 2012.